ORIGINAL ARTICLE

Fabrication of metal-organic framework Universitetet i Oslo-66 (UiO-66) and brown-rot fungus *Gloeophyllum trabeum* biocomposite (UiO-66@GT) and its application for reactive black 5 decolorization

Taufiq Rinda Alkas, Ratna Ediati, Taslim Ersam, Refdinal Nawfa, Adi Setyo Purnomo [*]

Department of Chemistry, Faculty of Science and Data Analytics, Institut Teknologi Sepuluh Nopember, Kampus ITS Sukolilo, Surabaya 60111, Indonesia

Abstract Many various industries use synthetic dyes as their raw materials. These dyes have triggered environmental problems because of the occurring effluents, and one of the environmentally safe solutions for this problem is biodegradation through microorganisms. Reactive Black 5 (RB5) dye degradation was performed by utilizing a metal-organic framework Universitetet i Oslo-66 (UiO-66) and *Gloeophyllum trabeum* (GT) fungus biocomposite. The UiO-66@GT composite was fabricated by inoculating the fungal culture in flasks with the PDB medium that contained UiO-66. This biocomposite was applied to decolorize and degrade RB5 dye, while pure GT culture can decolorize about 36.47% in five days. The percentage of RB5 decolorization was shown to be increased with the addition of UiO-66; the composite could decolorize RB5 up to 72.55% after five days incubation period. Moreover, the optimum conditions for the 100% targeted rate of RB5 decolorization found by the Response Surface Methodology (RSM) are: initial RB5 concentration (72.54 mg L^{-1}), pH (6.53), and temperature (38.06 °C). Two novel metabolites from RB5 decolorization by the composite were detected based on LCMS-QTOF analysis and were used to propose a degradation pathway: 6-((1-amino-7,8-dihydroxy-6-sulfonaphthalen-2-yl) diazinyl) cyclohexa-2,4-dien-1-ide (*m/z* = 360) and 3,4-diamino-5,6-dihydroxy-1,2,7,8-tetrahydronaphtha

[*] Corresponding author.
 E-mail addresses: adi_setyo@chem.its.ac.id, adi.spurnomo@yahoo.com (A.S. Purnomo).
Peer review under responsibility of King Saud University.

lene-2,7-disulfonic acid (m/z = 354).

1. Introduction

Dyes are essential materials broadly used across various aspects of life, ranging from textiles, paints, printing inks, food and beverages, pharmaceuticals, and cosmetics. As the usage of dyes increases yearly, there is also an increase in the production of dye waste by various industries (Wanyonyi et al., 2019). The textile industry uses synthetic dyes the most; it is estimated that around 15–50% of dyes are thrown out to the environment as wastewater during the synthesis and coloring process (Rehman et al., 2018; Vinayak and Singh, 2022). Moreover, its synthetic waste has various negative impacts on the environment and living organisms. For instance, in the aquatic environment, waste obstructs the entry of sunlight essential for photosynthesis, thereby affecting the availability of oxygen for plants and marine animals (Hassan and Carr, 2018). In addition, dye waste has not only toxic and non-degradable or recalcitrant properties but also allergic, mutagenic, and carcinogenic characteristics (Alam et al., 2021; Lellis et al., 2019; Wanyonyi et al., 2019).

One widely used synthetic dye of the "reactive" types is Reactive Black 5 (RB5), which has high water solubility and is most commonly used for coloring cotton, cellulosic fibers, wool, and nylon (Bilal et al., 2018; El Bouraie and El Din, 2016). However, this dye is a compound with highly toxic properties due to its non-degradable rigid aromatic molecules (Adnan et al., 2014). It has two azo bonds (-N = N-) with the potential to turn into toxic aromatic amines. According to Zille (2005), labile azo bonds enable enzymatic breakdown in mammals, including humans. Furthermore, the poisonous and carcinogenic properties of aromatic amines formed from the enzymatic breakdown depend on the 3-dimensional structure of the molecule and the location of its amine group. The European Chemical Agency (ECHA) states that RB5 may cause skin allergic reactions, allergy or asthma symptoms or breathing difficulties when inhaled (NCBI (PubChem), 2021). Meanwhile, in RB5 structures and other dyes, sulfonate groups have generally low potential to become genotoxic (Zille, 2005). Therefore, RB5 waste must be treated before being discharged into water bodies.

Various physiochemical methods have been developed to treat the dyes wastewater such as adsorption, filtration, sedimentation, photocatalytic, chemical oxidation, chemical coagulation and biological degradation (Maniyam et al., 2018; Tehubijuluw et al., 2021). Moreover, some of the downsides include high costs, low efficiency, limited usage, high amounts of energy, a lot of chemical uses, and generating a large volume of sludge (Singh, 2017; Benjamin and Ayinla, 2018; Oliveira et al., 2020; Sosa-Martínez et al., 2020). For example, RB5 absorption with activated carbon immobilized in cationic surfactants, a physical–chemical method, still required extremely acidic (pH 1.0–2.0) or basic (pH 11.0–12.0) conditions for high removal efficiency (Nabil et al., 2014). Jager et al. (2018) also reported that electrochemical oxidation methods almost completely remove colors within 15 min. However, as there is no aromatic and mineralization ring-opening process, the toxic property of the waste is still unchanged, and the by-product of hypochlorous acid is still corrosive. Thus, the biological/biodegradation method is an effective alternative with resilient adaptation, easy operation, environmentally-safe results, and lower (competitive) costs compared to physical and chemical methods (Maniyam et al., 2018; Wanyonyi et al., 2019).

One of the microorganisms widely used in bioremediation is fungi, which have high resistance to various pollutants and can degrade some pollutants such as dyes (Nabilah et al., 2022). White rot fungus is commonly applied in the degradation of a variety of pollutants research and well-known as a commercial enzymes producer for dye degrada-

tion (Singh, 2017). In addition, brown-rot fungi (BRF) have also been applied to the biodegradation of various pollutants, including synthetic dyes. BRF have been tested to break down organic pollutants such as TNT, chlorophenol, fluoroquinolone, aldrin, dieldrin, DDT, and stains (Purnomo et al., 2019). One of BRF species, *Gloeophyllum trabeum*, reportedly produces an essential enzyme laccase for generating the hydroxyl radicals which play an important role in degradation process (Arimoto et al., 2015; Csarman et al., 2021). This enzyme has robust capabilities in degrading phenolic and non-phenolic compounds (Debnath and Saha, 2020). *G. trabeum* fungus has been investigated for its RB5 degrading ability by Hartikainen et al. (2016). However, this result was not highlighted as it did not show its decolorization capabilities in solid media (Malt Extract Agar).

Meanwhile, Purnomo et al. (2020) reported that *G. trabeum*, with the addition of Fe^{2+}, degraded methyl orange dyes by 46.67% on liquid Mineral Salt Medium (MSM). The research also proved the mechanism of the Fenton reaction in *G. trabeum* metabolic activity, which produces hydroxyl radicals. Moreover, the Fenton reaction effectively degrades various hazardous materials and organic pollutants through its catalytic oxidation process using hydrogen peroxide and ferrous ions (Fe^{2+}) to produce OH radicals (Purnomo et al., 2019). These hydroxyl radicals attack dye molecules either in azo or hydrazo tautomer form, breaking N = N or C-N bonds sequentially (Santos et al., 2021). The facts above show that *G. trabeum* fungus can degrade synthetic dyes but still require modification to improve the degradation process.

In the bioremediation method, microorganisms are used to eliminate pollutants in the environment using the mechanism of absorption and degradation with the help of enzymes. Furthermore, Hassan and Carr (2018) stated that dye decolorization was caused by biomass absorption and degradation of dye chromophores by enzymes. Legerská et al. (2016) also confirmed that degradation of azo dyes by laccase enzyme occurs by an asymmetric breakdown of azo bonds followed by other reactions, such as oxidative breakdown, desulphonation, deamination, demethylation, and dehydroxylation, whereby such response depends on the chemical structure of the dye. However, the use of microorganisms, specifically fungi, in this method still has limitations, including the need for low pH conditions, long growth phases, long hydraulic retention periods for decolorization, and large reactor sizes (Arikan et al., 2019). An effort to overcome this problem is combining fungal culture with other materials to increase its effectiveness. In addition, it aims to produce a physically supports for microorganisms to maintain their enzymatic activity and more resilience to environmental disturbance such as physical stressing and pH/toxic effect (Diorio et al., 2021).

Several supporting materials have been reported to have biocompatible properties, including loofah sponge, alginate, corncobs, and Macro Porous Polymeric Sponge (MPPS). Additionally, Laraib et al. (2020) reported the using loofah sponge matrix for the fungus *Aspergillus tereus*, where decolorization of the dyes Congo red successively reached 92% within 24 h at 100 ppm. Methylene blue (MB) and Malachite green (MG) dye removal show the results of 7,400 mmol/g and 5 mmol/g, respectively. In line with this, Zhang et al. (2017) reported using corncobs as a fungal matrix where decolorization reaches 80% at pH 4.5–5. Li et al. (2018) also said immobilization of the fungus *Phanerochaete chrysosporium* with sodium alginate (2% w/v) to remove Cr(III), Acid Violet 7, and Basic Fuchsin, confirming that it can remove Cr(III) binary pollutants and dyes. Arikan et al. (2019)

immobilized *Penicillium glabrum* with MPPS, found the highest percentage of textile industry wastewater decolorization reaching 98.2% with batch reactors.

Another material that can be combined with fungal culture is a metal–organic framework (MOF), previous works use MOF as a supporting material for enzymes. For example, the laccase enzyme plays an essential role in dye decolorization. It has been combined with several types of MOF, including UiO-66 (Wu et al., 2022), ZIF-8 (Mahmoodi and Abdi, 2019), and MIL-68 (Peng et al., 2021). Those reports prove that MOF can be a supporting matrix for fungal enzymes. MOF materials have the advantage of good stability at various pH (Schelling et al., 2018), high thermal stability, large surface area, high porosity, and resilience in water media (Ediati et al., 2019). In this research, MOF type UiO-66 is used as supplementary material for *G. trabeum* fungus, which produces laccase enzyme. Some studies reported the absorption ability of MOF UiO-66 for dyes (Azhar et al., 2017; Jiang et al., 2019), and micropollutants in water (Schelling et al., 2018).

Meanwhile, optimization techniques by experiencing each factor consume a long time and are too expensive (Das and Mishra, 2017). Furthermore, finding the optimum condition for the decolorization process requires an evaluation of different parameters which potentially affect the result (Mahmoudian et al., 2021). Therefore, this present study uses the statistical method response surface methodology (RSM) to predict the optimum condition and determine the relationship between response and a set of factors. A practical and essential technique such as RSM is also helpful for designing the experiments. This tool can be utilized to assess the effect of process factors and their connection to process response. The relationship was presented in an equation model for forecasting the response by various conditions.

This research aims to fabricate and characterize a new biocomposite of UiO-66@GT and investigate its ability to decolorize RB5 dye. Considering other studies, we expect accelerated dye adsorption by UiO-66, supported by the biodegradation process by *G. trabeum* fungus. In this study, the measurements of the isothermal and thermodynamic adsorption aspects of these materials were also conducted. The effects of several variables such as initial dye concentration, pH, and temperature were evaluated, and the RSM tool analyzed the optimum condition. Furthermore, the metabolite products and the degradation pathway of the RB5 decolorization were also predicted based on the result of the LCMS-QTOF analysis.

2. Experimental

2.1. Materials

G. trabeum NBRC 6509 (NITE Biological Resource Center, Chiba, Japan) culture stock was obtained from the collection of Microbial Chemistry Laboratory, Institut Teknologi Sepuluh Nopember. Stock cultures were propagated on PDA solid medium (Potato Dextrose Agar; Merck) and then on PDB liquid medium (Potato Dextrose Broth; HiMedia). Reactive Black 5 (RB5) dye was supplied from Sigma Aldrich (Germany), and the physicochemical properties are shown in Table 1. UiO-66 was synthesized in the laboratory using the solvothermal method (Pambudi et al., 2021).

2.2. Fabrication of G. trabeum and UiO-66 composite

One petri dish of *G. trabeum* culture (in PDA medium) and 25 mL of demineralized water were blended using a Waring blender with a sterilized cup. Then one milliliter of the homogenate was injected into several Erlenmeyer containing 20 mL of potato dextrose broth and UiO-66 with varying masses (15, 30, and 45 mg). Subsequently, the mixture was incubated and

horizontally slowly shaken at $\pm$ 35 °C for three days. After three days, the granules that emerged were washed aseptically with sterile water ($\pm$ 20 mL) to remove the liquid medium. The UiO-66@GT biocomposite was characterized by SEM, XRD, and FTIR spectrophotometer.

2.3. Decolorization test

UiO-66@GT biocomposite was added to a flask containing 10 mL of RB5 solution with a concentration of 100 mg L^{-1} then incubated under static conditions. Afterwards, sample decolorization was observed and measured after 1, 3, and 5 days. The sample was centrifuged at 3000 rpm for 10 min, and the supernatant was analyzed using a UV–vis spectrophotometer (Thermo Genesys-10S) in the range of 300–800 nm. The percentage of decolorization was calculated from the absorbance of the sample at the maximum wavelength (λ max), based on equation (1):

$$\% \text{ Decolorization (PD)} = \frac{Abs_0 - Abs_t}{Abs_0} x 100\% \tag{1}$$

where Abs_0 and Abs_t are respectively control and treatment absorbances (Purnomo et al., 2019). Biocomposite variation with the highest decolorization percentage was used for further testing.

2.4. Various effects of parameters on dye decolorization

Several parameters investigated for their effect in the decolorization include initial pH, temperature, and dye concentration. First, variations in pH conditions were evaluated by giving 100 mg L^{-1} concentration of RB5 solution at various pH (3–13) regulated by adding HCl or NaOH into Erlenmeyers containing biocomposite. The same applies to the other parameter variations, namely temperature (25–45 °C) and the initial concentration of RB5 (100, 150, 200, 250, and 500 mg L^{-1}). Meanwhile, all Erlenmeyer containing the dye solution and the biocomposite were incubated for three days. Finally, the supernatant was carefully removed from the centrifuged solution, decanted, and analyzed with UV–vis and FTIR spectrophotometer.

2.5. Adsorption experiments

Determination of the adsorption capacity of UiO-66 and UiO-66@GT composite used the RB5 dye solution with concentration 100 mg L^{-1}. 20 mL of this solution was poured into an Erlenmeyer containing UiO-66 (0.5 g L^{-1}) or composite UiO-66@GT (50 g L^{-1}) and placed in a shaker at 120 rpm and temperature of 30 °C. The adsorption capacity of the material is determined using the equation (2):

$$q_t = \frac{(C_0 - C_t) \times V}{W} \tag{2}$$

where q_t is the adsorption capacity (mg g^{-1}), C_0 is the initial RB5 concentration, C_t is the final concentration at time t (mg L^{-1}), V is the volume of adsorbate (L), and W is the mass of the adsorbent (g). After the adsorption process in the various times, the samples were centrifuged at 3000 rpm to separate the solution from the adsorbent. Then the absorbance

Table 1 General characteristics of Reactive Black 5 dye.

Properties	Information
IUPAC Name	tetrasodium;4-amino-5-hydroxy-3,6-bis[[4-(2-sulfonatooxyethylsulfonyl)phenyl]diazenyl]naphthalene-2,7-disulfonate
C.I. name / number	Remazol Black 5 / 13,657,666
Commercial name	Reactive Black 5
CAS number	17095–24-8
Melting point	> 300 °C
Density	1.21 g/cm^3 at 20 °C
Chemical Safety (GHS Hazard statements)	H317: May cause an allergic skin reaction
	H334: May cause allergy or asthma symptoms or breathing difficulties if inhaled
Molecular weight	991.8
Molecular formula	$C_{26}H_{21}N_5Na_4O_{19}S_6$
Chemical stucture	
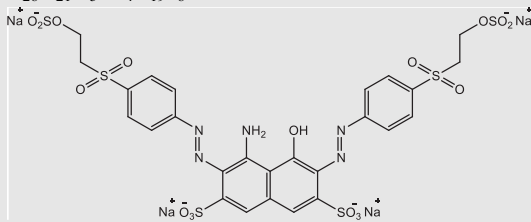
was measured with a UV–Vis spectrophotometer at the maximum wavelength to find out the concentration of the solution.

2.5.1. Isothermal adsorption

Meanwhile, to define the type of isothermal adsorption that occurs, variation of concentrations 50, 100, 150, 200, 250, and 500 mg L^{-1} of RB5 dye were tested. After being added to the Erlenmeyer containing the tested material, the mixture was shaken under the same conditions and measured at equilibrium time. Next, the data are fitted to the Langmuir model (Eq. (3)) and the Freundlich model (Eq. (4)), and the determination of the appropriate model was through the correlation coefficient (R^2). The equations of the two models are as follows (Hidayat et al., 2021):

$$\frac{1}{q_e} = \frac{1}{q_m \times K_L \times C_e} + \frac{1}{q_m} \qquad (3)$$

$$\ln q_e = \ln K_F + \frac{1}{n} \ln C_e \qquad (4)$$

where C_e (mg L^{-1}) is the concentration of RB5 at equilibrium; q_e (mg g^{-1}) is adsorption capacity at equilibrium; q_m is the maximum adsorption capacity; K_L represented Langmuir's constant; K_F represented the Freundlich constant; and n^{-1} represented the heterogeneity factor of the adsorption strength.

2.5.2. Adsorption thermodynamics

For finding the thermodynamic aspects in this study, RB5 dye concentration of 100 mg L^{-1} was used. The condition was regulated by shaking at 120 rpm and using the temperature variations of 293.15, 303.15, and 313.15 K. Gibbs free energy (ΔG), entropy change (ΔS), and enthalpy change (ΔH) are also determined using the equilibrium constant (K_d, Eq. (7)) and obtained from equation (6). The parameters ΔH and ΔS were calculated via equation (5), so the value of ΔG can be determined by the Van't Hoff equation (Dali Youcef et al., 2019):

$$\ln K_d = \frac{\Delta S}{R} + \frac{\Delta H}{RT} \qquad (5)$$

$$\Delta G = \Delta H - T\Delta S \qquad (6)$$

$$K_d = \frac{q_e}{C_e} \qquad (7)$$

where K_d is the distribution coefficient of the adsorption; ΔH denoted enthalpy; ΔS denoted entropy; ΔG represented the Gibbs free energy; T was the experimental temperature (K); and R is the ideal gas constant.

2.6. Optimization of RB5 decolorization condition by RSM

This study applied mathematical and statistical methods used to make the decolorization process model by UiO-66@GT. Response surface methodology (RSM) is a tool from the exact sciences attributed to the suitability of empirical models and the gained experimental data in relation to experimental design, and finding the connection between the response and the independent variables is the aim of this method (Mazarji et al., 2017). Toward this aim, three factors were designed as independent variables, namely initial dye concentration (X_1), pH (X_2), and temperature (X_3). Using Box-Behnken experimental design, RSM was applied to study those effects on RB5 decolorization. This design requires a practical number of runs (N, Eq. (8)) according to Das and Mishra (Das and Mishra, 2017):

$$N = K^2 + K + C_P \qquad (8)$$

Where K is the total of factors (3 factors), and Cp is the center point adjusted to 3; thus, the total runs were 15 experimental runs. Design Expert software version 13.0.5.0 was utilized in this experiment to analyze them and predict the optimum condition. Three factorial variables consist of initial dye concentration (50, 100, and 150 mg L^{-1}), pH (4, 7, and 10), and temperature (25, 35, and 45 °C). Table 2 presents those variables, and the levels as follows:

The dependent variable of this research is the decolorization rate. Experimental result was fitted into a second-order equation (9):

Table 2 Symbols and variables code for RB5 decolorization using Box-Behnken design.

Independent Variables	Symbol	Levels		
		low (-1)	middle (0)	high (+1)
Initial dye concentration (mg L^{-1})	X_1	50	100	150
pH	X_2	4	7	10
Temperature (°C)	X_3	25	35	45

$$y = \beta_0 + \beta_1 X_1 + \beta_2 X_2 + \beta_3 X_3 + \beta_{11} X_1^2 + \beta_{22} X_2^2$$
$$+ \beta_{33} X_3^2 + \beta_{12} X_1 X_2 + \beta_{13} X_1 X_3 + \beta_{23} X_2 X_3 \quad (9)$$

where y is a response of RB5 decolorization percentage, β_0, β_1, β_2, and β_3 are linear interaction coefficients; β_{11}, β_{22}, and β_{33} relate to the quadratic coefficients. In addition, β_{12}, β_{13}, and β_{23} denote the interaction coefficients, while X_1, X_2, and X_3 designate as independent variables.

3. Result and discussion

3.1. Characterization of UiO-66 and UiO-66@GT composite

This research combines UiO-66 as an effective adsorbent material with *G. trabeum* fungus, which produces the laccase enzyme. This enzyme was practically used as a degrading agent for Reactive Black 5 dye. Moreover, the addition of MOF UiO-66 to the grown fungus at the incubation time makes round granules (composite) in shaking conditions. The structure of this composite was evaluated by XRD and FTIR, whereby the XRD diffractogram showed high and moderate-intensity peaks at several angles of 2Θ (7.16°, 8.33°, and 25.53°) in Fig. 1**a**. It was almost similar to the characteristic peaks of UiO-66 reported by Hidayat et al. (2021) and Li et al. (2019). However, the intensity decreased drastically after combining with *G. trabeum* in the UiO-66@GT composite. These results still indicated that the structure of UiO-66 in this composite was relatively stable, which was proven by its octahedral shape on the UiO-66@GT SEM micrographs (Fig. 3c).

Meanwhile, the FTIR spectrum, depicted in Fig. 1**b**, illustrated the difference between UiO-66 and UiO-66@GT. There was a broad O-H peak at 3406 cm^{-1} of the carboxylate group, indicating the O-H stretching vibrational mode from benzene dicarboxylic acid which is the organic linker on the UiO-66 structure. The peak at 1657 cm^{-1} was associated with C=O stretching on the carboxylate group, similarly to Pambudi et al. (2021) and Hidayat et al. (2021). Characteristically, the peak between 1350 and 1700 cm^{-1} belonging to asymmetric and symmetric stretching of carboxylic functional groups (Molavi et al., 2018). At the same time, the strong peak at 1398 cm^{-1} was ascribed to the C-O bond of C-OH group of carboxylic acid. According to Pambudi et al. (2021), the peaks at 551 and 746 cm^{-1} were related to Zr-O's bending and stretching modes.

The visual appearance of *G. trabeum* and UiO-66 composite was shown in Fig. 2**a**, and the composite formed a round granule in PDB media; fungal mycelia also grew on the flask wall. In addition, the fungal mycelium formed spherical granules during the incubation by the shaking treatment and became the sheets when the liquid medium was removed (Fig. 2**c**). The applied composite for decolorizing RB5 is depicted in Fig. 2**b**. In submerged cultures, the fungi form a pellet consisting of dense agglomerates of hyphae that may be spherical or ellipsoidal agglomerates (Ibrahim, 2015). Therefore, this indicates that shaking treatment in the fungal growth could make the culture turn to a spherical form and entrap any surrounding materials.

Moreover, the morphological analysis of the composite by Scanning Electron Microscope (SEM) showed a spherical form of the composite and the fibrous cross-section of the fungus to which the MOF was bonded (Fig. 3**a and 3c**). The SEM micrograph also showed UiO-66 granules spread on *G. trabeum*
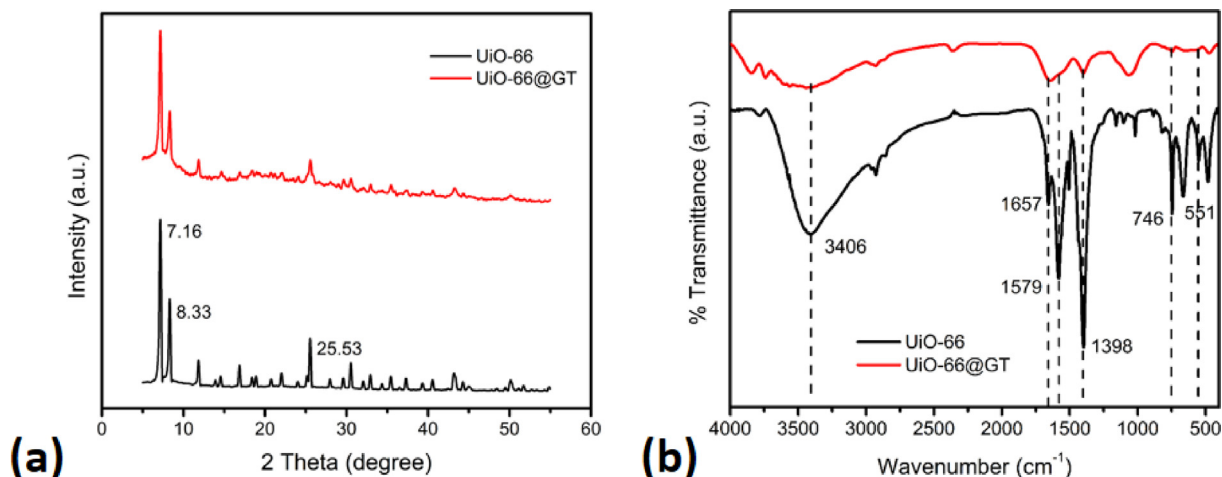
Fig. 1 Characteristic of UiO-66 and UiO-66@GT composite: (a) XRD Diffractogram, (b) FTIR spectra.
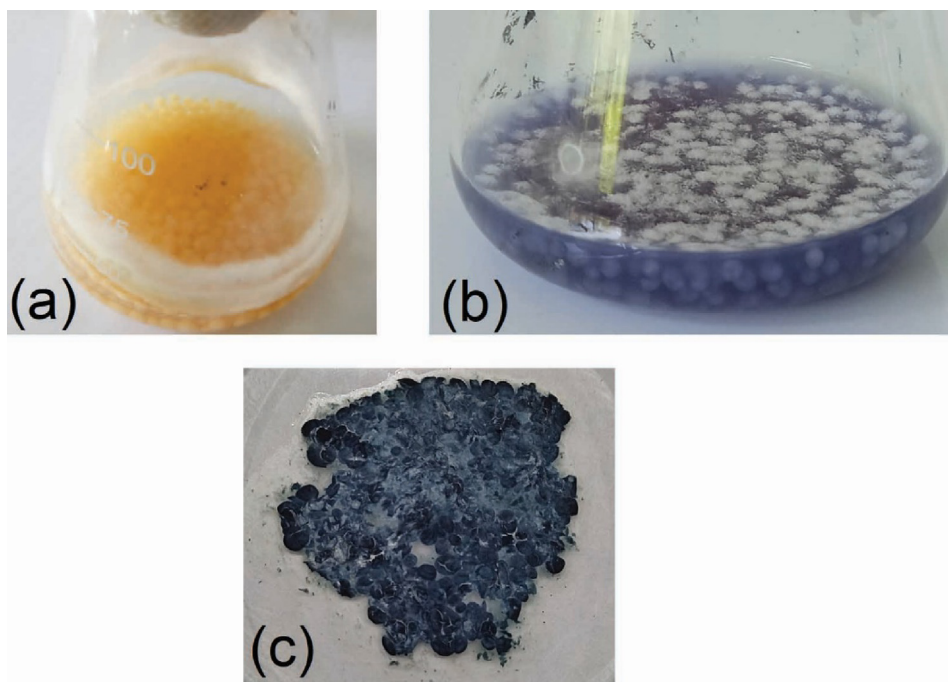
Fig. 2 (a) UiO-66@GT appearance after three days incubation, (b) UiO-66@GT composite at five days decolorization time, and (c) the filtered composite after five days used.

hyphae surface (Fig. 3b). Rosário et al. (2019) similarly discovered that particulate Ln-MOFs accumulate uniformly along with the whole tubular cell of *Aspergillus niger*, which inoculated in a sterile solution containing glucose and Ln-MOF. As a result, entrapped Ln-MOFs are discovered and firmly bound over the fungal surface. In this research, UiO-66, added to the culture media containing *G. trabeum* fungus, was dispersed either on the surface or within the granules by shaking condition.

The composite granules had different diameter sizes; the diameter of the UiO-66@GT composite in Fig. 3a is approximately 2.6 mm. Ibrahim (2015) also discovered that the fungal mycelia turned to form a few spherical and elongated pellets of fungal growth at 200 rpm with sizes between 0.6 and 1.0 mm at the shaking condition. Meanwhile, this structure still allows the dye to be absorbed into the MOF UiO-66. According to Ediati et al. (2021), UiO-66 has the potential role as a promising adsorbent because it has various advantages such as large surface area, high porosity, and stability in water. In addition, the composite structure permitted the enzyme activity to be more efficient because of the substrate (RB5) was accumulated on the adsorbent.

3.2. Decolorization of Reactive Black 5

The transformation of the RB5 profile with a concentration of 100 mg L^{-1} by MOF UiO-66 and UiO-66@GT biocomposite was shown in Fig. 4. Adsorption is the primary mechanism of UiO-66 in this decolorization process; indications of degradation do not occur since there is no significant pattern change of the UV–vis profile over time (Fig. 4a). On the other hand, the UV–vis spectrum of RB5 decolorization with the biocomposite (Fig. 4b, line of Day 1–5) showed a different shape from the RB5 control curve (black line), specifically at a wavelength

of around 300 nm, which may indicate there is a degradation process by the composite.

In addition, the FTIR profile in Fig. 4c also supports the statement that the composite has degraded RB5 dye. The supernatant samples were shown different peaks compared to the IR spectrum band of RB5, mainly in the range of 1500–1000 cm^{-1}. Aromatic C=C vibrations at 1635 cm^{-1} were still noticeable in the IR spectra of composite and pure fungi. The missing peaks, such as C-O stretch at 1222 cm^{-1} and S=O vibration of 1134 cm^{-1} from the sulphonate group, indicated that RB5 was degraded. The fact of RB5 characteristic peaks disappearance was a sign of the degradation process that was also found by Bilal et al. (2018), Martorell et al. (2017), and El Bouraie and El Din (2016).

The percentage of RB5 decolorization by UiO-66 increased with the accumulation of contact time and stopped after the MOF was saturated. Moreover, the decolorization percentage by UiO-66 reached a maximum value of 99.29% after 48 h of incubation (Table 3). Electrostatic interactions explain the connection between the dye and UiO-66 or UiO-66@GT. Since RB5 has the sulfonic groups, it behaves like anions in the solution and UiO-66 with Zr^{4+} as the central atom with a positive charge. Similarly, Bouras et al. (2019) found that the decolorization of dyes by the composites of dead fungi (*Aspergillus carbonarius* and *Penicillium glabrum*) with ZnO through an adsorption mechanism, where Reactive Red 180 dye, which has a sulfonate group (-SO$_3^-$) interacts with a group of ZnO present in ZnO/AC and ZnO/PG composites. Therefore, electrostatic interactions occurred, and the appearance of aromatic benzenes in both also allows π-π interactions to arise.

Pure UiO-66 has a high level of decolorization to RB5 dye (99.29%). Still, the contribution of adsorption ability in the UiO-66@GT biocomposite was not significant, and this may
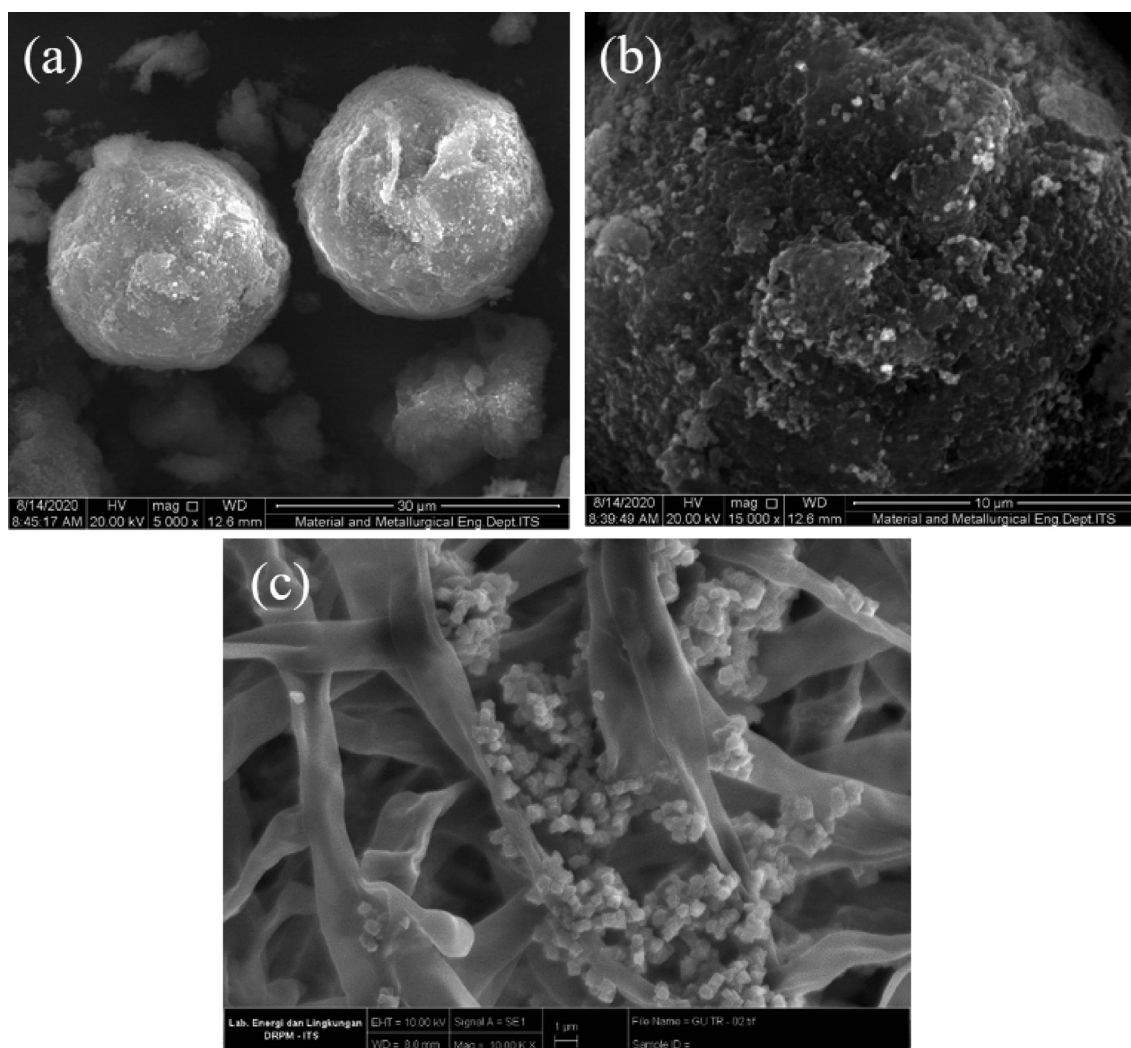
Fig. 3 SEM Micrographs: (a) spherical granules of UiO-66@GT composite (magnified 5K x), (b) the composite surface (magnified 15K x), (c) cross-section of the composite (magnified 10K x).

occur due to the closure of pores partially or even entirely by the fungal hyphae. Furthermore, *G. trabeum* still grows even though it has been combined with UiO-66 as a biocomposite. After several days, mycelia *G. trabeum* could still proliferate on the solution's surface. This may be a drawback for its application in a reactor because it causes clogging. This problem may be solved in upcoming research.

In addition, Table 4 shows the percentage of decolorization of pure *G. trabeum* culture and UiO-66@GT biocomposite. Pure culture of *G. trabeum* had a decolorization rate of 36.47 ± 0.78% after five days of incubation, and the lesser enzyme production causes this low achievement. However, UiO-66@GT (15 mg) was the lowest decolorization rate, possibly due to the minimum amount of UiO-66 and the lower production of the laccase enzyme. On the other hand, it was found that the variation of *G. trabeum* and 30 mg UiO-66 had the highest reaching (72.55 ± 0.41%), and this composition was used in further experiments. This chosen composition was evaluated in several states to determine the optimum decolorization condition, such as initial dye concentration, pH, and temperature.

3.3. Initial concentration effect on dye decolorization

The initial concentration effect was evaluated by varying the concentration of RB5 in the range of 100–500 mg L^{-1} into a flask containing UiO-66@GT (30 mg) biocomposite. After the sample was incubated under static conditions, there was a significant decrease (Fig. 5a), where the sample with RB5 concentration of 100 mg L^{-1} showed maximum decolorization rate (53.97 ± 0.91%) after three days of incubation. Meanwhile, the percentage dropped to a minimum of 500 mg L^{-1} (2.33 ± 1.81%). That fact asserts the decolorization of RB5 will be diminished as an increasing initial dye concentration.

The toxicity of RB5 is the logical reason why the decrease occurs in this biocomposite, and it may trigger a terminated or inactive state. Strengthening that statement, Kunjadia et al. (2016) have reported that total decolorization efficiency declines above 100 ppm dye concentration and the phenomenon arises due to inhibition for growing cells by dye toxicity limiting nucleic acid biosynthesis. Another previous study by Chen and Ting also revealed the efficiency of dye decolorization at lower initial dye concentrations (50 and
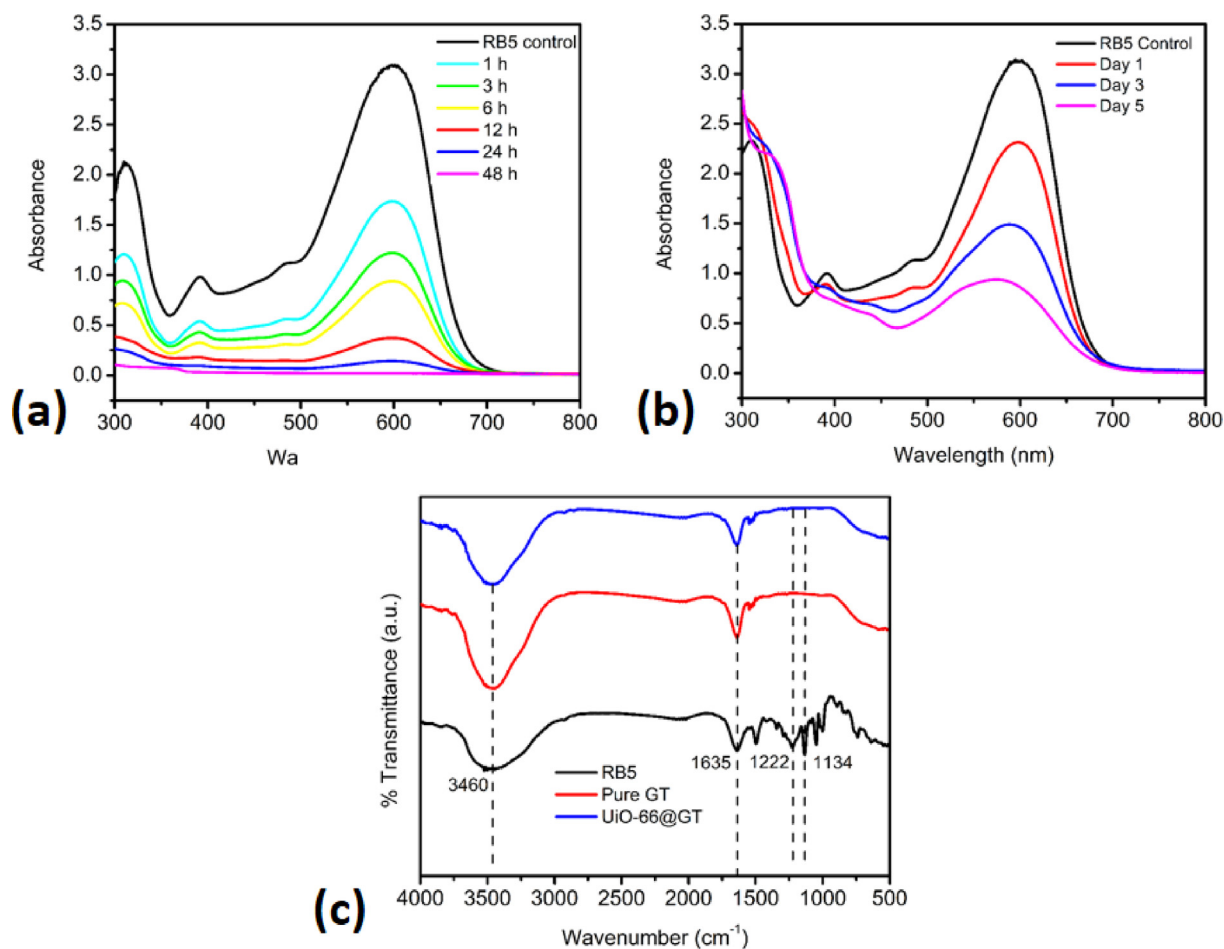
Fig. 4 UV–vis profile of RB5 decolorization after five days incubation by a. UiO-66; b. UiO-66@GT; and c. FTIR spectra of RB5 standard and RB5 decolorization supernatant by pure GT and UiO@GT.

Table 3 Reactive Black 5 decolorization by UiO-66.

Contact time (hours)	% Decolorization*
1	43.94 ± 1.39[a]
3	60.61 ± 2.49[b]
6	69.65 ± 1.76[b]
12	87.90 ± 0.71[c]
24	95.36 ± 2.54[c]
48	99.29 ± 0.05[c]

*The data were calculated from the absorbances of the samples of UV–vis Spectrophotometer at λmax. It presented as the mean ± standard deviations (n = 2). Additionally, the different lower letters indicated the significant difference using statistical analysis T-test at various contact times of UiO-66 ($p < 0.05$).

100 mg L^{-1}) higher than 200 mg L^{-1} (Chen and Yien Ting, 2015). Similarly, Ortiz-Monsalve et al. (2017) found that dye decolorization by the Brazilian native white-rot fungi strains of *Trametes villosa* reached high biodecolorization (over 90%) at lower concentration (100–300 mg L^{-1} for Acid Red

357, Acid Black 210, and Acid Blue 161 dyes. At higher concentrations (600–1000 mg L^{-1}), the fungus required a longer incubation time to gain the same biodecolorization efficiency. They also stated an increase in the dye concentrations reduced the biodecolorization capacity because the higher concentrations are toxic to microorganisms, inhibiting fungal growth and obstructing the enzymes activities. In addition, Varjani et al. (2020) stated that high dye concentration can influence dye degradation by blocking the enzyme sites. Therefore, the higher concentrations required a longer decolorization period than the lower dye concentrations.

3.4. pH effect on dye decolorization

One of the essential factors for fungi is pH, a crucial parameter for growth and the enzyme's production in many biodegradations. In this context, the different pH showed various decolorization results. This study examined the pH range 3 to 13 and found that the maximum pH for decolorizing RB5 by the composite was 11. The UiO-66@GT biocomposite achieved the maximum decolorization rate at pH 11, while at pH 3 the dye solution produced a minimum value (Fig. 5b). After three days of incubation, the UiO-66@GT composite at pH 11 could reach 42.63 ± 0.46%. This condition was also similar to the activated carbon from an almond shell, which is

Table 4 Decolorization percentages of RB5 by pure Gt and UiO-66@GT composite.

Day	% Decolorization			
	Pure Gt	UiO-66@GT (15 mg)	UiO-66@GT (30 mg)	UiO-66@GT (45 mg)
1	27.10 ± 2.83^a	23.29 ± 1.87^a	26.37 ± 0.07^a	16.93 ± 4.52^b
3	35.55 ± 6.65^a	25.21 ± 2.03^a	53.97 ± 0.91^b	39.21 ± 6.62^b
5	36.47 ± 0.78^a	26.53 ± 3.08^a	72.55 ± 0.41^b	52.68 ± 1.62^c
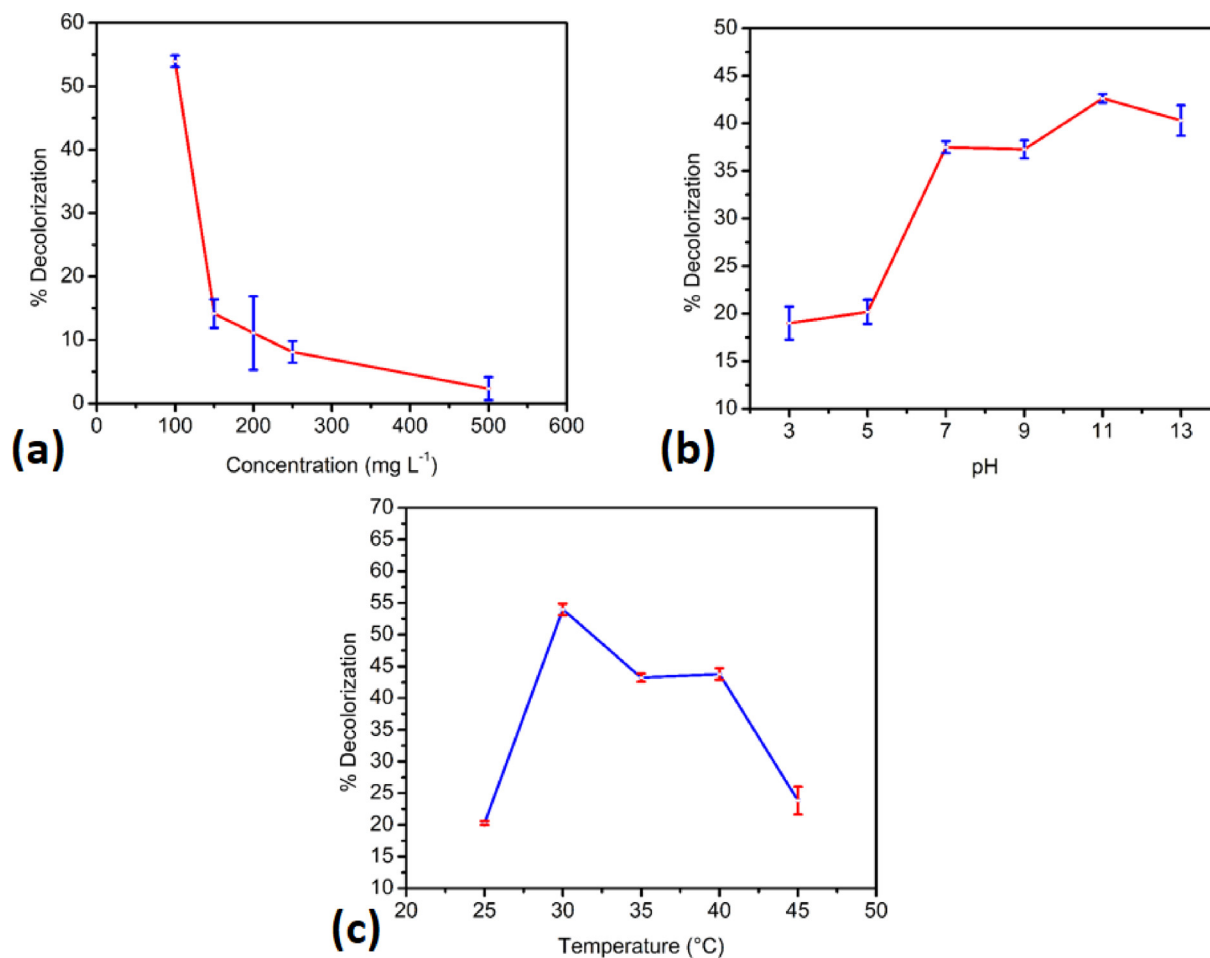
Fig. 5 (a) Initial concentration effect, (b) pH effect, and (c) temperature effect on RB5 decolorization after three days contact time.

used to remove rhodamine B; it achieved a maximum color removal percentage of about 70% at pH 11 (Abdolrahimi and Tadjarodi, 2019). Therefore, decolorization by the composites tends to be optimum in the alkaline range, but above pH 11, the rate was decreased.

In addition, laccase which is produced by *G. trabeum* metabolism has an essential role in dye degradation, has a specific pH for its synthesis. For example, in the case of *Trametes polyzona* fungus, Ezike et al. (2020) found the maximum laccase activity in the acidic region (pH 4.5) than in the neutral/alkaline region. While at higher pH than 6.5, they cannot observe the laccase activity. Previous study showed the maximum laccase activity value after three days incubation was 222.23 IU mL^{-1} at pH 5.5 for *Trametes hirsuta* and also exhibited a maximum decolorization (84.81%) of Reactive Brilliant Blue R (RBBR) (Bibi and Bhatti, 2012). While Wanyonyi et al. (2019) found the maximum decolorization of RB5 (98%) observed at pH 9 by a crude protease extract from *Bacillus cereus*. However, pH factor did not only affect the enzyme production but also contributed to physical and chemical interactions between dyes and adsorbents. Our research also found that *G. trabeum* fungus on immobilized form showed the highest decolorization of RB5 at pH 3.0 due to the electrostatic interaction between the anionic dye and protonated adsorbent (Alkas et al., 2022).

According to Kaushik and Malik (2009), the optimal pH for fungi to predominate in dye decolorization is in the acidic range, but this low pH is not suitable for wastewater

treatment. Furthermore, various pH of the textile waste and its multiple compositions might be challenging to control in the acid range, and it will be more expensive. Therefore, a prerequisite for fungi that can be applied in wastewater treatment is the ability to grow in a wide range of pH and degrade effluents (Gomaa et al., 2011). This composite (UiO-66@GT) has the opportunity to be a potential degrader for this reason. Still, it must be modified to overcome drawbacks such as a longer time to complete degradation, clogging issues, and resilience.

3.5. Temperature effect on dye decolorization

Another essential aspect is temperature, which is also required by every microorganism to grow normally. Sadhasivam et al. (2008) found that laccase produced by *Trichoderma harzianum* WL1 fungus was active in the temperature range of 30–50 °C, with optimal activity at 35 °C. Another study using *Aspergillus flavus* and *Penicillium canescens* discovered that 30 °C and 35 °C were the most efficient temperatures in direct blue decolorization, respectively (Hefnawy et al., 2017). However, Afreen et al. (2018) claimed the temperature effect is very significant for enzyme activity. The dye's decolorization level is affected by fungal growth and supported within a limited temperature range. At a higher temperature, there will be a reduction in decolorization rate due to the loss of cell sustainability or denaturation of the active enzymes. On the other hand, Bankole et al. (2019) reported that *Aspergillus niger* could decolorize the thiazole yellow G dye perfectly at the different temperature (40 °C); they also explained the decolorization process by the fungi usually declines with the increasing temperature. Moreover, laccase, as an essential enzyme for dye degradation, also has the highest activity at 40 °C and its activity vanished at 60 °C which has been reported by Pandi et al. (2019) from a novel fungal strain *Peroneutypa scoparia*.

In this work, the dye degradation process by UiO-66@GT composite obtained the highest result at a temperature of 30 °C, shown in Fig. 5c. After 30 °C, the composite decolorization ability decreased, which may be due to the fungal cell inactivation or the enzyme deactivation. At the same time, UiO-66 surface area and pores were not mainly roled in here because of its closure by the fungal's mycelia.

3.6. Adsorption experiments

3.6.1. Isothermal adsorption
Based on the adsorption data, the isothermal adsorption model of UiO-66 and UiO-66@GT was shown in Fig. 6. Both materials have the same isothermal adsorption model (Langmuir model), it seen from the value of the correlation coefficient (R^2) both were greater than the value in the Freundlich model. The R^2 values of both were 0.9344 and 0.9619, respectively, indicating that the two materials followed the Langmuir model where RB5 adsorption occurs on the surface of the monolayer material. Meanwhile, from interpolating the data into equations (3) and (4), other parameters were obtained as in Table 5. The maximum adsorption capacity (q_m) of UiO-66 material was much greater than that of the UiO-66@GT composite, namely 133,333 and 0.390 mg L^{-1}, respectively. The drastic decrease from the original capacity of UiO-66 with UiO-66@GT composite was caused by the pores closure or

UiO-66 entrapment in the fungal mycelia, so that the active site that could bind the dye was reduced.

Furthermore, the higher q_m of UiO-66 than the composite proved that the decolorization ability of UiO-66 was much better than the composite. It is proven that within 24 h the decolorization rate of RB5 with UiO-66 can reach 95.36%, while the composite only reaches 26.37%. In addition, the adsorption contribution in the percentage of decolorization of fungal composites was lower than the metabolic activity of fungi. Similarly, Barapatre et al. (2017) who found that the color reduction contribution from absorption was only ~ 2–3% of the decolorization of Malachite green (MG) dye that occurred, the rest was the metabolic activity of the fungus.

3.6.2. Adsorption thermodynamics
To understand the adsorption process and the mechanism of RB5 adsorption by UiO-66 and UiO-66@GT, it is necessary to look for its thermodynamic parameters. The adsorption process was carried out at various temperatures of 293.15, 303.15, and 313.15 K, from the results of handling experimental data obtained into equations (5) and (6) then the values of ΔG, ΔH, and ΔS were known as in Table 6. The ΔG value of both UiO-66 and UiO-66@GT obtained negative values, indicating that the RB5 dye adsorption was a spontaneous process. Both materials showed that the effect of increasing temperature on the value of ΔG, the spontaneous adsorption goes up with the increasing temperature of the system. Meanwhile, the negative ΔH values of UiO-66 and its composites were −53,486 and −16,930 kJ mol-1, respectively, indicating the exothermic nature of the adsorption. Batouti et al. (2022) mentioned that if ΔH$_{ads}$ values are −4 to −40 kJ mol^{-1} it will be physisorption ranges, but from −40 to −800 kJ mol^{-1} is chemisorption. And from this point, we can classify that the RB5 adsorption by UiO-66 was chemisorption and the UiO-66@GT composite was physisorption (See Table 6).

However, the exothermic adsorption property was also found in methyl orange (MO) dye, Molavi et al. (2018) stated that the interaction between MO dyes and UiO-66 could be due to dentate exchange and/or dipole-dipole interactions. Similarly, obtained by Tian et al. (2021) with another type of MOF MIL-101(Cr)–NH$_2$ in adsorbing Sb(III), also obtained positive ΔS values as in this study. A positive ΔS value indicates the irregularity and randomness of the adsorbate at the solid-liquid interface which increases during adsorption.

3.7. Optimization condition using RSM

The decolorization test for this optimization was performed for five days; the lowest and highest percentages from the running experiments were 9.60 and 92.53 percent, respectively. By the Box-Behnken design, 15 experiment variation were conducted, it was found a second order (quadratic) polynomial equation which fitted to this experimental data as written as follow (Eq. 10):

$$y = 81.55 - 36.89X_1 + 1.48X_2 - 0.73X_3 + 0.27X_1X_2$$
$$- 1.83X_1X_3 - 4.05X_2X_3 + 6.02X_1^2 - 34.27X_2^2$$
$$- 30.33X_3^2 \tag{10}$$
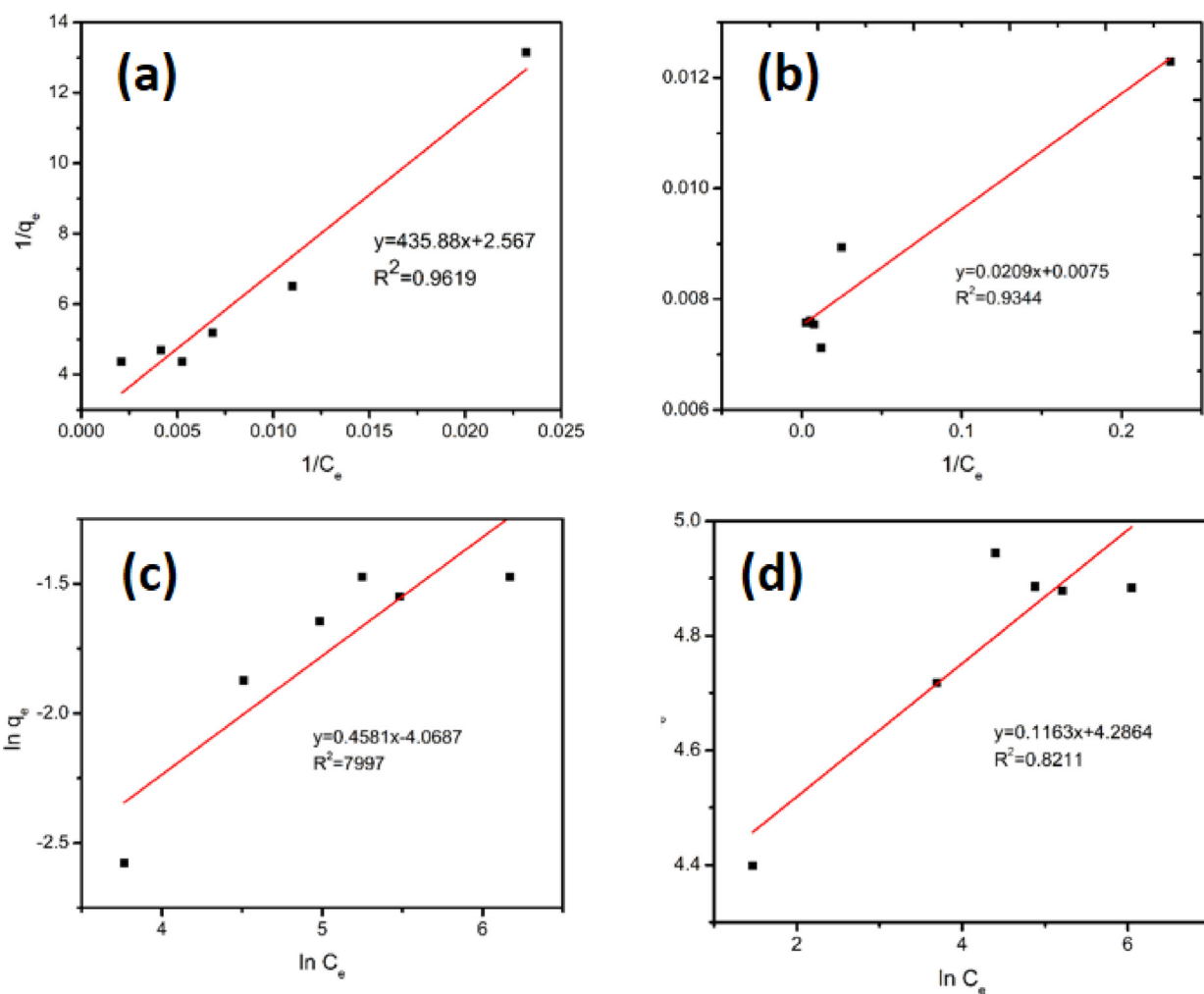
Fig. 6   Langmuir models: (a) UiO-66@GT; (b) UiO-66; Freundlich models: (c) UiO-66@GT; and (d) UiO-66.

Table 5   Parameters related to isotherm models of RB5 adsorption by UiO-66 and UiO-66@GT.

Langmuir model				Freundlich model			
Adsorbent	R^2	q_m	K_L	Adsorbent	R^2	n^{-1}	K_F
UiO-66	0.9344	133.333	0.359	UiO-66	0.8211	0.116	72.704
UiO-66@GT	0.9619	0.390	0.006	UiO-66@GT	0.7997	0.458	0.017

Table 6   Thermodynamic parameters on the adsorption of RB5 by UiO-66 and UiO-66@GT composites.

Adsorbents	T (K)	ΔG (kJ mol^{-1})	ΔH (kJ mol^{-1})	ΔS (J (mol K)$^{-1}$)
UiO-66	293.15	−104.184	−53.486	172.940
	303.15	−105.913		
	313.15	−107.642		
UiO-66@GT	293.15	−17.965	−16.930	3.532
	303.15	−18.000		
	313.15	−18.036		
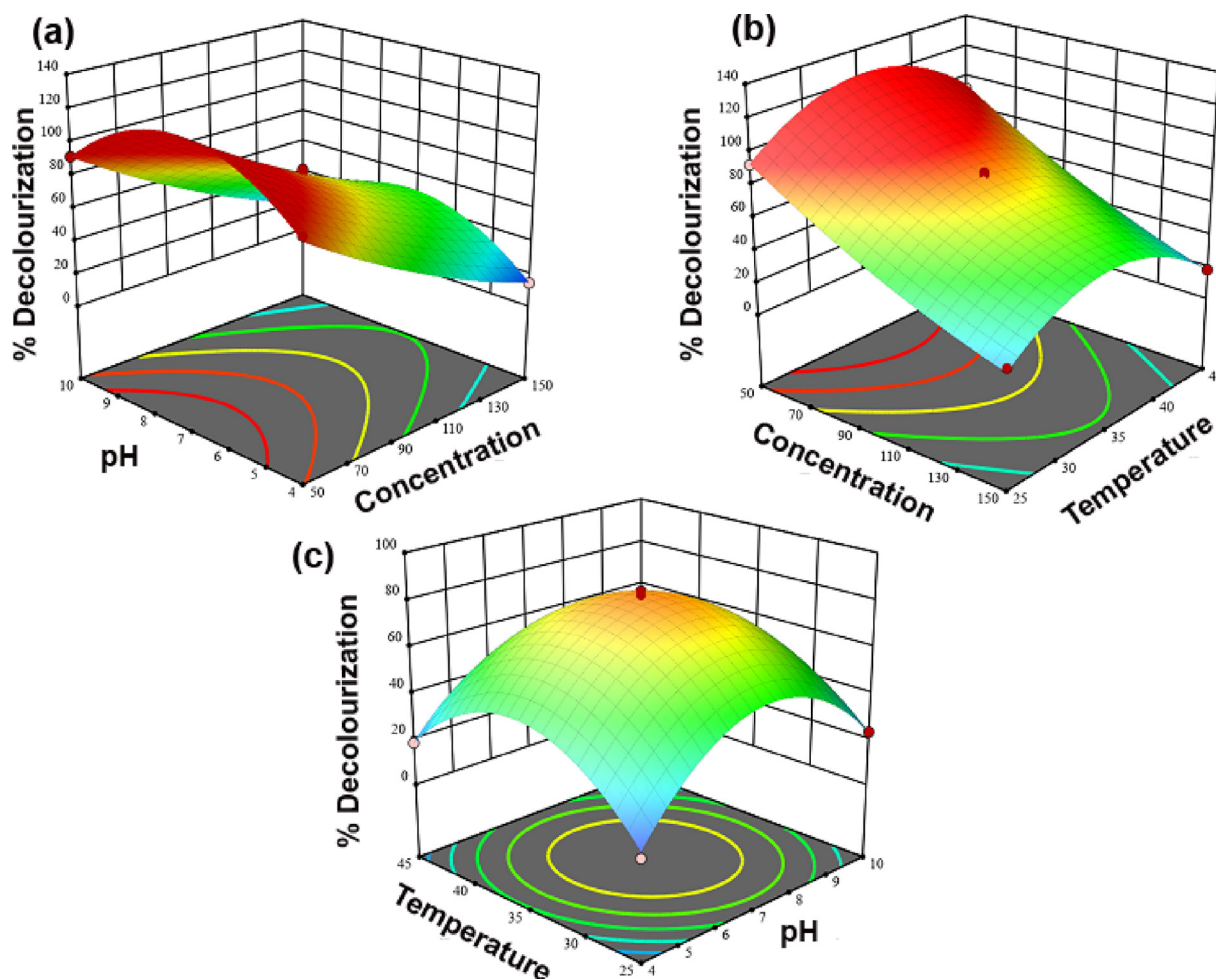
Fig. 7 Three-dimensional response surface plot for the effect of (a) pH and concentration, (b) Concentration and Temperature, (c) Temperature and pH.

The values of X_1, X_2, and X_3 in this study have been adjusted and listed in Table 2. The significance of the quadratic polynomial suitable for the RB5 decolorization percentage was evaluated by performing an analysis of variance (ANOVA). The high F-value of this model of 156.09 and the lack of fit F-value of 1.81 showed the model was a good fit. The model also has a p-value < 0.05 (< 0.0001), indicating that the model is significant.

The correlation coefficient (R^2) is defined as the ratio of the explained variation to the overall variation and denotes a measure of the goodness of fit. A good model fit is expected to produce an R-squared value of at least 0.8 (Figueiredo Filho et al., 2011). Thus, this model with an R-squared of 0.9965 indicates a high degree of correlation between the observed and predicted responses. The adjusted R-squared value is near the predicted R-squared: 0.9901 and 0.9564, respectively, showing the acceptability of the model.

The ultimate aim of the response surface model in this study is to find out the optimum condition of RB5 decolorization by the UiO-66@GT composite. The response surface graphs are depicted in Fig. 7. These response surface plots are supportively to understand the interactive effects of two variables. For instance, Fig. 7a shows the interaction between concentration and pH, and the RB5 decolorization will be higher if the dye concentration is 50 mg L^{-1} and pH is about 7. Similarly, from Fig. 7c, an increased decolorization rate will occur if the solution is nearly pH 7 and the temperature is around 35 °C. And using Design Expert 13.0.5.0 version, the experimental data appropriately fitted into the equation (10), and the condition for 100% targeted rate of RB5 decolorization are initial RB5 concentration (72.54 mg L^{-1}), pH (6.53), and temperature (38.06 °C). Unfortunately, after trying a decolorization test by the condition, the result could not achieve a nearly 100% (69.62%) decolorization rate due to the difference between the actual condition.

3.8. LC-MS analysis

The mass spectrum of the metabolites of RB5 degradation by the UiO-66@GT biocomposite was shown in Fig. 8. In this research, the instrument was unable to show the specific peaks of the molecular structure of the dye RB5 ($m/z = 991$), and Wanyonyi et al. (2019) observed the same; they suggest this due to the direct dissociation of RB5 when dissolved in water. According to the chromatogram and mass spectrum analysis, two new metabolites were detected at 1.28 mins with $m/z = 360$ and predicted as 6-((1-amino-7,8-dihydroxy-6-sulfo

Table 7 Various metabolic/degradation products of RB5 by several studies.

Treatment	Metabolic products (molecular weight (MW) or m/z)	Structures	References
Bacterial biodecolorization *Rhodopseudomonas palustris*	MW = 200.89 and 347.13		Wang et al., 2008
Degradation by immobilized bacteria *Aeromonas punctate* in calcium alginate bead	MW = 172		Usha et al., 2012
Degradation by fungus *Trametes gibbosa* sp.	m/z = 73		Adnan et al., 2014
Oxidation using TiO_2/WO_3 nanostructured photoanode under visible light irradiation	m/z = 706; 436; and 200		Guaraldo et al., 2016
Degradation by bacteria *Aeromonas hydrophila*	m/z = 349 and 280		El Bouraie and El Din, 2016
Degradation by yeast *Trichosporon akiyoshidainum*	m/z = 279.98		Martorell et al., 2017
Degradation induced by UV/TiO_2	MW = 346; 189; and 90		Bilal et al., 2018
Degradation by crude Protease enzyme from *Bacillus cereus*	m/z = 295.14; 98.96; and 144.08		Wanyonyi et al., 2019
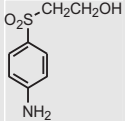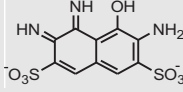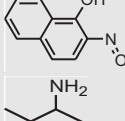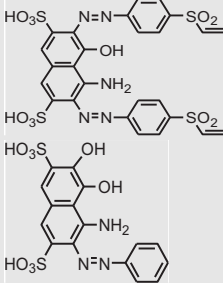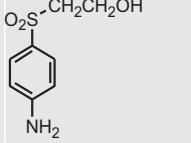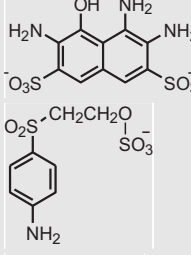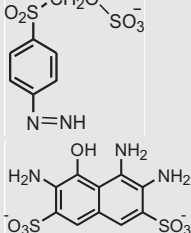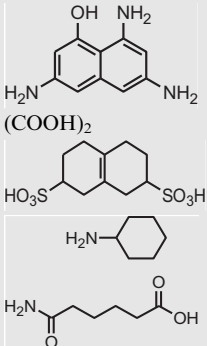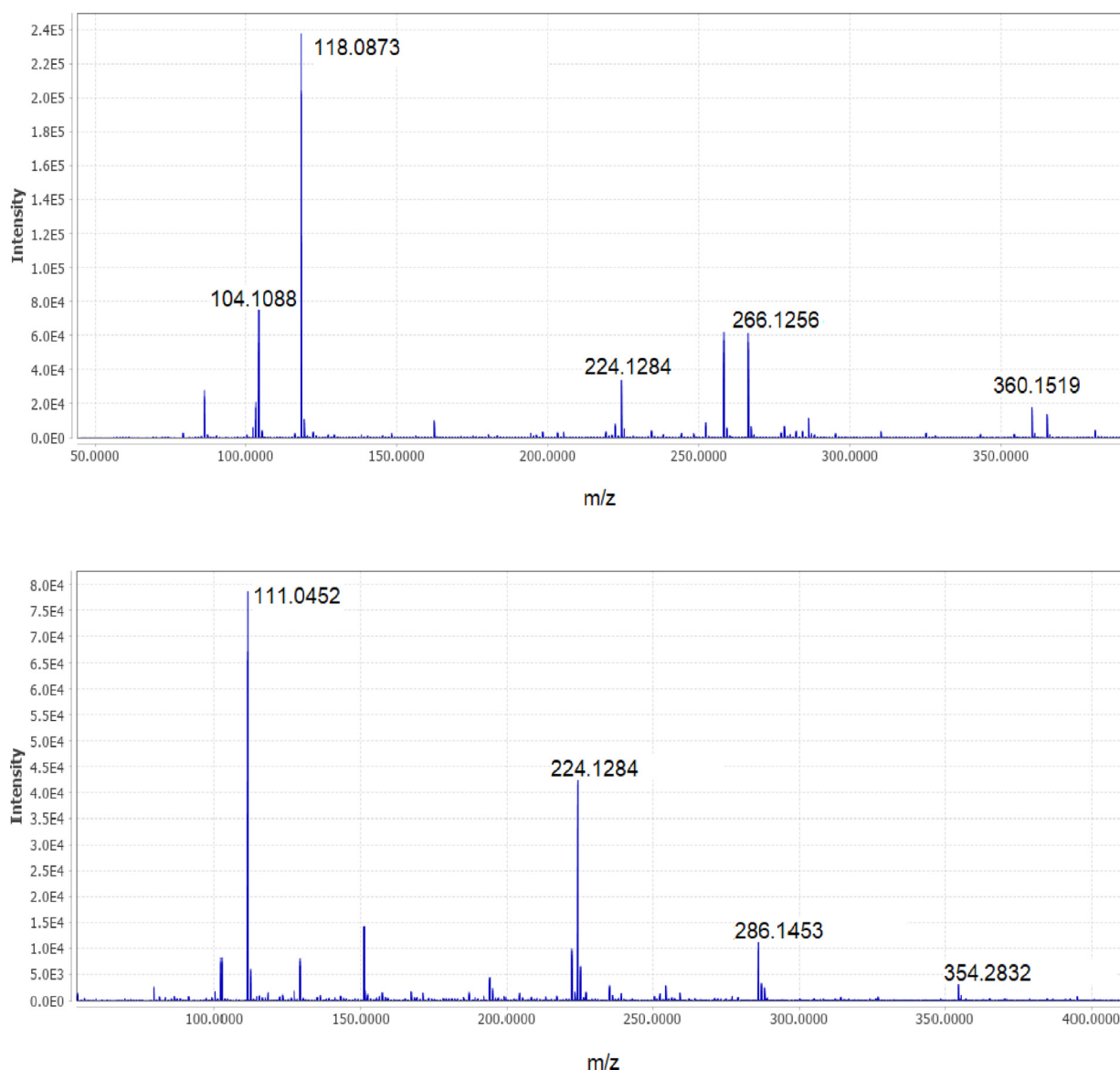
Fig. 8 Mass spectrum of product metabolites of RB5 decolorization: (a) $m/z = 360$, (b) $m/z = 354$.

naphthalen-2-yl) diazinyl) cyclohexa-2,4-dien-1-ide. At the same time, the second compound was detected at 2.76 mins with $m/z = 354$ and predicted as 3,4-diamino-5,6-dihydroxy-1,2,7,8-tetrahydro-naphthalene-2,7-disulfonic acid.

Meanwhile, these two discovered metabolites with $m/z = 360$ and 354 were analyzed by LCMS-QTOF equipment. To predict the structure of these results, this study refers to Guaraldo et al. (2016) that discovered $m/z = 706$ as one of the degradation products of RB5. Furthermore, their research proposed a degradation pathway that also found $m/z = 436$ as one of the by-products. This molecule resulted from desulphonation and hydroxylation mechanisms splitting the $m/z = 706$ ions. Although chromatograms and mass spectra cannot detect these peaks, they were used to propose a RB5 degradation pathway and corresponding metabolite products.

Several researchers have identified metabolic products of RB5 biodegradation (Adnan et al., 2014; El Bouraie and El Din, 2016; Martorell et al., 2017; Usha et al., 2012; Wang et al., 2008; Wanyonyi et al., 2019). Besides fungi and bacteria, several treatments have been applied for degrading RB5 dye (Bilal et al., 2018; Guaraldo et al., 2016). Table 7 shows RB5 metabolic products from various RB5 degradation research. This research also offers a new degradation pathway of RB5 by UiO-66@GT composite, which is shown in Fig. 9. Afterward, the RB5 molecule may be changed to $m/z = 706$ by enzymatic or Fenton reactions because BRF has the most significant asset (Fenton reaction), generating hydroxyl radicals. It suggests that the $m/z = 706$ molecule reacts with a hydroxyl radical to form the $m/z = 354$ ions and the product developed by asymmetric cleavage, hydrogenation, and the Fenton reaction. The other ($m/z = 360$) was formed by the enzymatic metabolism (laccase) of $m/z = 436$. This metabolite is produced by subsequent desulphonation of $m/z = 436$ to the ion $m/z = 360$. In addition, Legerská et al. (2016) also described the degradation of azo dyes by laccase starting with asymmetric cleavage of the azo bond followed by oxidative
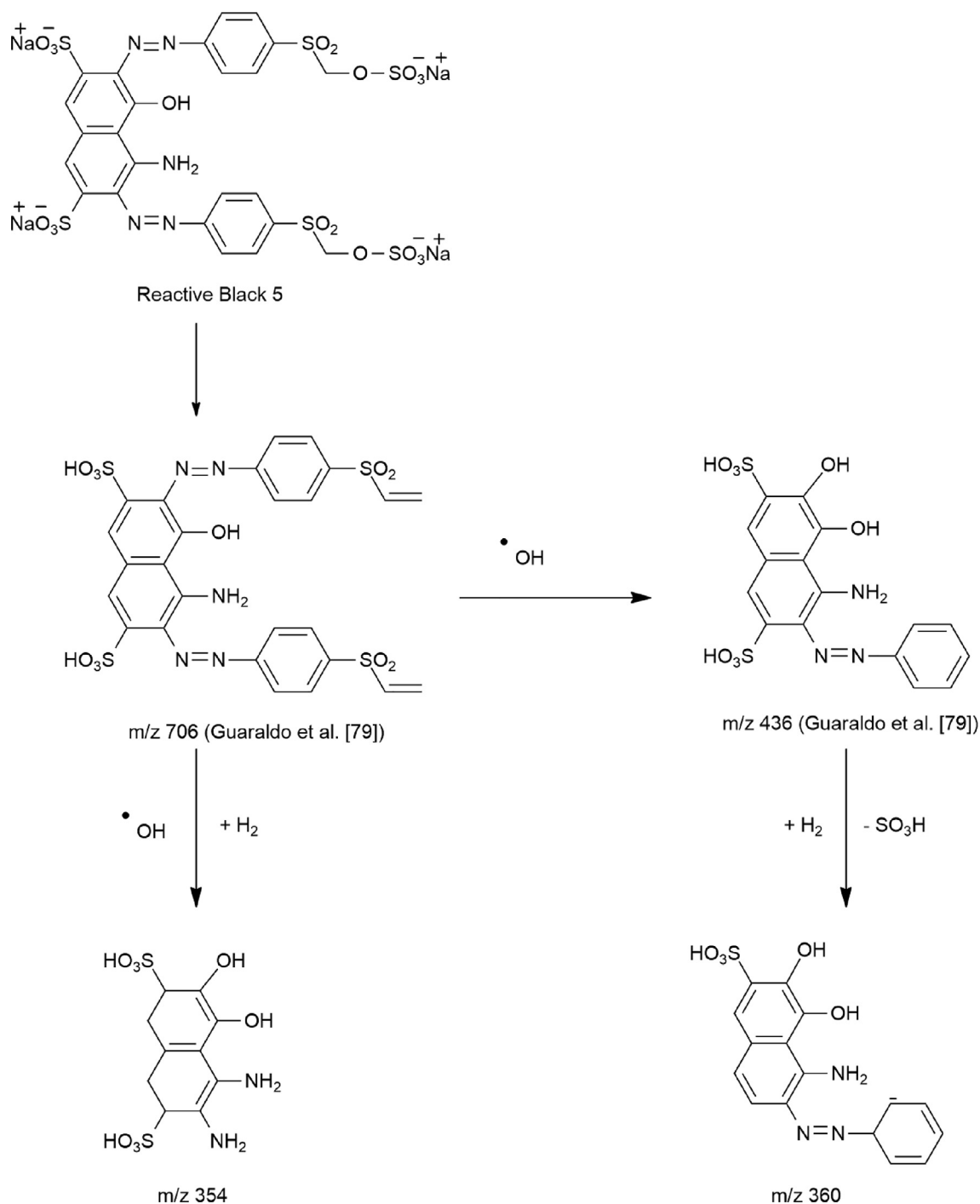
Fig. 9 Proposed pathway of RB5 degradation by UiO-66@GT.

cleavage, desulphonation, deamination, demethylation, and dehydroxylation, depending on the structure of the dye.

4. Conclusions

In summary, a biocomposite of MOF UiO-66 and *G. trabeum* fungus was successfully fabricated and proven to degrade Reactive Black 5 dye (72.55%) better than pure cultures of *G. trabeum*. By evaluating a single parameter effect to decolorization test, it was found the maximum condition as follows: initial dye concentration of 100 mg L^{-1}; pH 11; and 30 °C. On the other hand, by using the RSM tool, the condition for the 100% targeted rate of RB5 decolorization were an initial RB5 concentration of 72.54 mg L^{-1}, pH value of 6.53, and a temperature 38.06 °C. Furthermore, the novel metabolites from RB5 decolorization using the LCMS-QTOF analysis were detected, namely 6-((1-amino-7,8-dihydroxy-6-sulfonaphthalen-2-yl) diazinyl) cyclohexa-2,4-dien-1-ide (m/z = 360) and 3, 4-diamino-5,6-dihydroxy-1,2,7,8-tetrahydronaphthalene-2,7-disulfonic acid (m/z = 354) and a new pathway of RB5 transformation by UiO-66@GT composite was proposed.

Declaration of Competing Interest

Acknowledgements

References

Abdolrahimi, N., Tadjarodi, A., 2019. Adsorption of Rhodamine-B from Aqueous Solution by Activated Carbon from Almond Shell, in. In: The 23rd International Electronic Conference on Synthetic Organic Chemistry. Presented at the International Electronic Conference on Synthetic Organic Chemistry, p. 51. https://doi.org/10.3390/ecsoc-23-06619.

Adnan, L.A., Mohd Yusoff, A.R., Hadibarata, T., Khudhair, A.B., 2014. Biodegradation of Bis-Azo dye Reactive Black 5 by White-Rot Fungus Trametes gibbosa sp. WRF 3 and its metabolite characterization. Water. Air. Soil Pollut. 225, 2119. https://doi.org/10.1007/s11270-014-2119-2.

Afreen, S., Anwer, R., Singh, R.K., Fatma, T., 2018. Extracellular laccase production and its optimization from Arthrospira maxima catalyzed decolorization of synthetic dyes. Saudi J. Biol. Sci. 25, 1446–1453. https://doi.org/10.1016/j.sjbs.2016.01.015.

Alam, R., Ardiati, F.C., Solihat, N.N., Alam, M.B., Lee, S.H., Yanto, D.H.Y., Watanabe, T., Kim, S., 2021. Biodegradation and metabolic pathway of anthraquinone dyes by Trametes hirsuta D7 immobilized in light expanded clay aggregate and cytotoxicity assessment. J. Hazard. Mater. 405,. https://doi.org/10.1016/j.jhazmat.2020.124176 124176.

Alkas, T.R., Ediati, R., Ersam, T., Purnomo, A.S., 2022. Reactive Black 5 decolorization using immobilized Brown-rot fungus Gloeophyllum trabeum. Mater. Today Proc. S2214785322011804. https://doi.org/10.1016/j.matpr.2022.02.521

Arikan, E.B., Isik, Z., Bouras, H.D., Dizge, N., 2019. Investigation of immobilized filamentous fungi for treatment of real textile industry wastewater using up flow packed bed bioreactor. Bioresour. Technol. Rep. 7,. https://doi.org/10.1016/j.biteb.2019.100197 100197.

Arimoto, M., Yamagishi, K., Wang, J., Tanaka, K., Miyoshi, T., Kamei, I., Kondo, R., Mori, T., Kawagishi, H., Hirai, H., 2015. Molecular breeding of lignin-degrading brown-rot fungus Gloeophyllum trabeum by homologous expression of laccase gene. AMB Express 5, 81. https://doi.org/10.1186/s13568-015-0173-9.

Azhar, M.R., Abid, H.R., Sun, H., Periasamy, V., Tadé, M.O., Wang, S., 2017. One-pot synthesis of binary metal organic frameworks (HKUST-1 and UiO-66) for enhanced adsorptive removal of water contaminants. J. Colloid Interface Sci. 490, 685–694. https://doi.org/10.1016/j.jcis.2016.11.100.

Bankole, P.O., Adekunle, A.A., Govindwar, S.P., 2019. Demethylation and desulfonation of textile industry dye, Thiazole Yellow G by Aspergillus niger LAG. Biotechnol. Rep. 23, e00327.

Barapatre, A., Aadil, K.R., Jha, H., 2017. Biodegradation of Malachite Green by the Ligninolytic Fungus Aspergillus flavus: general. CLEAN - Soil Air Water 45, 1600045. https://doi.org/10.1002/clen.201600045.

Batouti, M.E., Sadik, W., Eldemerdash, A.G., Hanafy, E., Fetouh, H.A., 2022. New and innovative microwave-assisted technology for synthesis of guar gum-grafted acrylamide hydrogel superabsorbent

for the removal of acid red 8 dye from industrial wastewater. Polym. Bull. https://doi.org/10.1007/s00289-022-04254-7.

Benjamin A, O., Ayinla, E., 2018. Effect of Nitrogen Source on Dye Decolouration by Alginate-immobilized Cells of Pseudomonas aeruginosa and Bacillus subtilis. Res. J. Environ. Sci. 12, 185–191. https://doi.org/10.3923/rjes.2018.185.191.

Bibi, I., Bhatti, H.N., 2012. Enhanced biodecolorization of Reactive Dyes by basidiomycetes under static conditions. Appl. Biochem. Biotechnol. 166, 2078–2090. https://doi.org/10.1007/s12010-012-9635-6.

Bilal, M., Rasheed, T., Iqbal, H.M.N., Hu, H., Wang, W., Zhang, X., 2018. Toxicological assessment and UV/TiO2-based induced degradation profile of Reactive Black 5 Dye. Environ. Manage. 61, 171–180. https://doi.org/10.1007/s00267-017-0948-7.

Bouras, H.D., Isik, Z., Bezirhan Arikan, E., Bouras, N., Chergui, A., Yatmaz, H.C., Dizge, N., 2019. Photocatalytic oxidation of azo dye solutions by impregnation of ZnO on fungi. Biochem. Eng. J. 146, 150–159. https://doi.org/10.1016/j.bej.2019.03.014.

Chen, S.H., Yien Ting, A.S., 2015. Biosorption and biodegradation potential of triphenylmethane dyes by newly discovered Penicillium simplicissimum isolated from indoor wastewater sample. Int. Biodeterior. Biodegrad. 103, 1–7. https://doi.org/10.1016/j.ibiod.2015.04.004.

Csarman, F., Obermann, T., Zanjko, M.C., Man, P., Halada, P., Seiboth, B., Ludwig, R., 2021. Functional expression and characterization of two laccases from the brown rot Fomitopsis pinicola. Enzyme Microb. Technol. 148,. https://doi.org/10.1016/j.enzmictec.2021.109801 109801.

Dali Youcef, L., Belaroui, L.S., López-Galindo, A., 2019. Adsorption of a cationic methylene blue dye on an Algerian palygorskite. Appl. Clay Sci. 179,. https://doi.org/10.1016/j.clay.2019.105145 105145.

Das, A., Mishra, S., 2017. Removal of textile dye reactive green-19 using bacterial consortium: process optimization using response surface methodology and kinetics study. J. Environ. Chem. Eng. 5, 612–627. https://doi.org/10.1016/j.jece.2016.10.005.

Debnath, R., Saha, T., 2020. An insight into the production strategies and applications of the ligninolytic enzyme laccase from bacteria and fungi. Biocatal. Agric. Biotechnol. 26,. https://doi.org/10.1016/j.bcab.2020.101645 101645.

Diorio, L.A., Fréchou, D.M.S., Levin, L.N., 2021. Removal of dyes by immobilization of Trametes versicolor in a solid-state micro-fermentation system. Rev. Argent. Microbiol. 53, 3–10. https://doi.org/10.1016/j.ram.2020.04.007.

Ediati, R., Setyani, M.A., Sulistiono, D.O., Santoso, E., Hartanto, D., Al Bakri Abdullah, M.M., 2021. Optimization of the use of mother liquor in the synthesis of HKUST-1 and their performance for removal of chromium (VI) in aqueous solutions. J. Water Process Eng. 39, 101670. https://doi.org/10.1016/j.jwpe.2020.101670.

Ediati, R., Zulfa, L.L., Nugroho, K.A., Mukminin, A., Sulistiono, D.O., Nadjib, M., Kusumawati, Y., 2019. One-pot solvothermal synthesis and characterization of UiO-66/HKUST-1 composites. IOP Conf. Ser. Mater. Sci. Eng. 578,. https://doi.org/10.1088/1757-899X/578/1/012072 012072.

El Bouraie, M., El Din, W.S., 2016. Biodegradation of Reactive Black 5 by Aeromonas hydrophila strain isolated from dye-contaminated textile wastewater. Sustain. Environ. Res. 26, 209–216. https://doi.org/10.1016/j.serj.2016.04.014.

Ezike, T.C., Ezugwu, A.L., Udeh, J.O., Eze, S.O.O., Chilaka, F.C., 2020. Purification and characterisation of new laccase from Trametes polyzona WRF03. Biotechnol. Rep. 28, e00566.

Figueiredo Filho, D.B., Silva Júnior, J.A., Rocha, E.C., 2011. What is R2 all about? Leviathan São Paulo 60. https://doi.org/10.11606/issn.2237-4485.lev.2011.132282.

Gomaa, O.M., Momtaz, O.A., Kareem, H.A.E., Fathy, R., 2011. Isolation, identification, and biochemical characterization of a brown rot fungus capable of textile dye decolorization. World J. Microbiol. Biotechnol. 27, 1641–1648. https://doi.org/10.1007/s11274-010-0618-x.

Guaraldo, T.T., Gonçales, V.R., Silva, B.F., de Torresi, S.I.C., Zanoni, M.V.B., 2016. Hydrogen production and simultaneous photoelectrocatalytic pollutant oxidation using a TiO2/WO3 nanostructured photoanode under visible light irradiation. J. Electroanal. Chem. 765, 188–196. https://doi.org/10.1016/j.jelechem.2015.07.034.

Hartikainen, E.S., Miettinen, O., Hatakka, A., Kähkönen, M.A., 2016. Decolorization of six synthetic dyes by Fungi. Am. J. Environ. Sci. 12, 77–85. https://doi.org/10.3844/ajessp.2016.77.85.

Hassan, M.M., Carr, C.M., 2018. A critical review on recent advancements of the removal of reactive dyes from dyehouse effluent by ion-exchange adsorbents. Chemosphere 209, 201–219. https://doi.org/10.1016/j.chemosphere.2018.06.043.

Hefnawy, M.A., Gharieb, M.M., Shaaban, M.T., Soliman, A.M., 2017. Optimization of culture condition for enhanced decolorization of direct blue dye by Aspergillus flavus and Penicillium canescens. J. Appl. Pharm. Sci. https://doi.org/10.7324/JAPS.2017.70210.

Hidayat, A.R.P., Sulistiono, D.O., Murwani, I.K., Endrawati, B.F., Fansuri, H., Zulfa, L.L., Ediati, R., 2021. Linear and nonlinear isotherm, kinetic and thermodynamic behavior of methyl orange adsorption using modulated Al2O3@UiO-66 via acetic acid. J. Environ. Chem. Eng. 9,. https://doi.org/10.1016/j.jece.2021.106675 106675.

Ibrahim, D., 2015. Effect of agitation speed on the morphology of Aspergillus niger HFD5A-1 hyphae and its pectinase production in submerged fermentation. World J. Biol. Chem. 6, 265. https://doi.org/10.4331/wjbc.v6.i3.265.

Jager, D., Kupka, D., Vaclavikova, M., Ivanicova, L., Gallios, G., 2018. Degradation of Reactive Black 5 by electrochemical oxidation. Chemosphere 190, 405–416. https://doi.org/10.1016/j.chemosphere.2017.09.126.

Jiang, D., Chen, M., Wang, H., Zeng, G., Huang, D., Cheng, M., Liu, Y., Xue, W., Wang, Z., 2019. The application of different typological and structural MOFs-based materials for the dyes adsorption. Coord. Chem. Rev. 380, 471–483. https://doi.org/10.1016/j.ccr.2018.11.002.

Kaushik, P., Malik, A., 2009. Fungal dye decolourization: recent advances and future potential. Environ. Int. 35, 127–141. https://doi.org/10.1016/j.envint.2008.05.010.

Kunjadia, P.D., Sanghvi, G.V., Kunjadia, A.P., Mukhopadhyay, P.N., Dave, G.S., 2016. Role of ligninolytic enzymes of white rot fungi (Pleurotus spp.) grown with azo dyes. SpringerPlus 5, 1487. https://doi.org/10.1186/s40064-016-3156-7.

Laraib, Q., Shafique, M., Jabeen, N., Naz, S.A., Nawaz, H.R., Solangi, B., Zubair, A., Sohail, M., 2020. Luffa cylindrica immobilized with Aspergillus terreus QMS-1: an efficient and cost-effective strategy for the removal of Congo Red using stirred tank reactor. Pol. J. Microbiol. 69, 193–203. https://doi.org/10.33073/pjm-2020-022.

Legerská, B., Chmelová, D., Ondrejovič, M., 2016. Degradation of synthetic dyes by laccases – a mini-review. Nova Biotechnol. Chim. 15, 90–106. https://doi.org/10.1515/nbec-2016-0010.

Lellis, B., Fávaro-Polonio, C.Z., Pamphile, J.A., Polonio, J.C., 2019. Effects of textile dyes on health and the environment and bioremediation potential of living organisms. Biotechnol. Res. Innov. 3, 275–290. https://doi.org/10.1016/j.biori.2019.09.001.

Li, C., Zhang, Y., Yong, M., Liu, W., Wang, J., 2019. Self-assembled membrane manufactured by metal–organic framework (UiO-66) coated γ-Al2O3 for cleaning oily seawater. RSC Adv. 9, 10702–10714. https://doi.org/10.1039/C9RA00521H.

Li, Y., Zheng, L., Li, Y., Dong, J., 2018. The simultaneous bioremoval of Cr(III) and dye by immobilized phanerochaete chrysosporium. J. Water Chem. Technol. 40, 108–115. https://doi.org/10.3103/S1063455X18020091.

Mahmoodi, N.M., Abdi, J., 2019. Metal-organic framework as a platform of the enzyme to prepare novel environmentally friendly nanobiocatalyst for degrading pollutant in water. J. Ind. Eng. Chem. 80, 606–613. https://doi.org/10.1016/j.jiec.2019.08.036.

Mahmoudian, F., Nabizadeh Chianeh, F., Sajjadi, S.M., 2021. Simultaneous electrochemical decolorization of Acid Red 33, Reactive Orange 7, Acid Yellow 3 and Malachite Green dyes by electrophoretically prepared Ti/nanoZnO-MWCNTs anode: experimental design. J. Electroanal. Chem. 884,. https://doi.org/10.1016/j.jelechem.2021.115066 115066.

Maniyam, M.N., Yaacob, N.S., Azman, H.H., Ab Ghaffar, N.A., Abdullah, H., 2018. Immobilized cells of Rhodococcus strain UCC 0004 as source of green biocatalyst for decolourization and biodegradation of methyl orange. Biocatal. Agric. Biotechnol. 16, 569–578. https://doi.org/10.1016/j.bcab.2018.10.008.

Martorell, M.M., Pajot, H.F., de Figueroa, L.I.C., 2017. Biological degradation of Reactive Black 5 dye by yeast Trichosporon akiyoshidainum. J. Environ. Chem. Eng. 5, 5987–5993. https://doi.org/10.1016/j.jece.2017.11.012.

Mazarji, M., Nabi-Bidhendi, G., Mahmoodi, N.M., 2017. One-pot synthesis of a reduced graphene oxide–ZnO nanorod composite and dye decolorization modeling. J. Taiwan Inst. Chem. Eng. 80, 439–451. https://doi.org/10.1016/j.jtice.2017.07.038.

Molavi, H., Hakimian, A., Shojaei, A., Raeiszadeh, M., 2018. Selective dye adsorption by highly water stable metal-organic framework: long term stability analysis in aqueous media. Appl. Surf. Sci. 445, 424–436. https://doi.org/10.1016/j.apsusc.2018.03.189.

Nabil, G.M., El-Mallah, N.M., Mahmoud, M.E., 2014. Enhanced decolorization of reactive black 5 dye by active carbon sorbent-immobilized-cationic surfactant (AC-CS). J. Ind. Eng. Chem. 20, 994–1002. https://doi.org/10.1016/j.jiec.2013.06.034.

Nabilah, B., Purnomo, A.S., Rizqi, H.D., Putro, H.S., Nawfa, R., 2022. The effect of Ralstonia pickettii bacterium addition on methylene blue dye biodecolorization by brown-rot fungus Daedalea dickinsii. Heliyon 8, e08963.

NCBI (PubChem), 2021. PubChem Compound Summary for CID 135442967, Reactive Black 5 [WWW Document]. Natl. Cent. Biotechnol. Inf. URL https://pubchem.ncbi.nlm.nih.gov/compound/Reactive-Black-5 (accessed 12.28.21).

Oliveira, J.M.S., de Lima e Silva, M.R., Issa, C.G., Corbi, J.J., Damianovic, M.H.R.Z., Foresti, E., 2020. Intermittent aeration strategy for azo dye biodegradation: A suitable alternative to conventional biological treatments? J. Hazard. Mater. 385, 121558. https://doi.org/10.1016/j.jhazmat.2019.121558.

Ortiz-Monsalve, S., Dornelles, J., Poll, E., Ramirez-Castrillón, M., Valente, P., Gutterres, M., 2017. Biodecolourisation and biodegradation of leather dyes by a native isolate of Trametes villosa. Process Saf. Environ. Prot. 109, 437–451. https://doi.org/10.1016/j.psep.2017.04.028.

Pambudi, M.A.R., Prayogo, N., Nadjib, M., Ediati, R., 2021. Study of UiO-66 and UiO-66 modulated with acetic acid as the adsorbent for Eriochrome Black T Dye. Indo. J. Chem. Res. 8, 183–193. https://doi.org/10.30598//ijcr.2021.8-riz.

Pandi, A., Marichetti Kuppuswami, G., Numbi Ramudu, K., Palanivel, S., 2019. A sustainable approach for degradation of leather dyes by a new fungal laccase. J. Clean. Prod. 211, 590–597. https://doi.org/10.1016/j.jclepro.2018.11.048.

Peng, J., Wu, E., Lou, X., Deng, Q., Hou, X., Lv, C., Hu, Q., 2021. Anthraquinone removal by a metal-organic framework/polyvinyl alcohol cryogel-immobilized laccase: effect and mechanism exploration. Chem. Eng. J. 418,. https://doi.org/10.1016/j.cej.2021.129473 129473.

Purnomo, A.S., Mauliddawati, V.T., Khoirudin, M., Yonda, A.F., Nawfa, R., Putra, S.R., 2019. Bio-decolorization and novel bio-transformation of methyl orange by brown-rot fungi. Int. J. Environ. Sci. Technol. 16, 7555–7564. https://doi.org/10.1007/s13762-019-02484-3.

Purnomo, A.S., Andyani, N.E.A., Nawfa, R., Putra, S.R., 2020. Fenton reaction involvement on methyl orange biodegradation by brown-rot fungus Gloeophyllum trabeum. In: Presented at the THE 14TH JOINT CONFERENCE ON CHEMISTRY 2019, p. 020002. https://doi.org/10.1063/5.0005230.

Rehman, K., Shahzad, T., Sahar, A., Hussain, S., Mahmood, F., Siddique, M.H., Siddique, M.A., Rashid, M.I., 2018. Effect of Reactive Black 5 azo dye on soil processes related to C and N cycling. PeerJ. 6, 1–14. https://doi.org/10.7717/peerj.4802.

Rosário, J., da Luz, L.L., Geris, R., Ramalho, J.G.S., da Silva, A.F., Júnior, S.A., Malta, M., 2019. Photoluminescent organisms: how to make fungi glow through biointegration with lanthanide metal-organic frameworks. Sci. Rep. 9, 7302. https://doi.org/10.1038/s41598-019-43835-x.

Sadhasivam, S., Savitha, S., Swaminathan, K., Lin, F.-H., 2008. Production, purification and characterization of mid-redox potential laccase from a newly isolated Trichoderma harzianum WL1. Process Biochem. 43, 736–742. https://doi.org/10.1016/j.procbio.2008.02.017.

Santos, P.B., Dos Santos, H.F., Andrade, G.F.S., 2021. Photodegradation mechanism of the RB5 dye: A theoretical and spectroscopic study. J. Photochem. Photobiol. Chem. 416,. https://doi.org/10.1016/j.jphotochem.2021.113315 113315.

Schelling, M., Kim, M., Otal, E., Hinestroza, J., 2018. Decoration of cotton fibers with a water-stable metal-organic framework (UiO-66) for the decomposition and enhanced adsorption of micropollutants in water. Bioengineering 5, 14. https://doi.org/10.3390/bioengineering5010014.

Singh, L., 2017. Biodegradation of synthetic dyes: a mycoremediation approach for degradation/decolourization of textile dyes and effluents. J. Appl Biotechnol. Bioeng. 3. https://doi.org/10.15406/jabb.2017.03.00081.

Sosa-Martínez, J.D., Balagurusamy, N., Montañez, J., Peralta, R.A., Moreira, R. de F.P.M., Bracht, A., Peralta, R.M., Morales-Oyervides, L., 2020. Synthetic dyes biodegradation by fungal ligninolytic enzymes: Process optimization, metabolites evaluation and toxicity assessment. J. Hazard. Mater. 400, 123254. https://doi.org/10.1016/j.jhazmat.2020.123254.

Tehubijuluw, H., Subagyo, R., Yulita, M.F., Nugraha, R.E., Kusumawati, Y., Bahruji, H., Jalil, A.A., Hartati, H., Prasetyoko, D., 2021. Utilization of red mud waste into mesoporous ZSM-5 for methylene blue adsorption-desorption studies. Environ. Sci. Pollut. Res. 28, 37354–37370. https://doi.org/10.1007/s11356-021-13285-y.

Tian, T., Jia, Y., Wu, J., Zhao, J., Xu, K., Wang, Z., Wang, Z., 2021. Effective adsorption of antimony(III) by MIL-101(Cr)-NH2: influencing-factor and characterization analyses and response surface optimization. Desalination Water Treat. 244, 226–240. https://doi.org/10.5004/dwt.2021.27898.

Usha, M.S., Sasirekha, B., Bela, R.B., Devi, S., Kamalini, C., Manasa, G.A., Neha, P.M., 2012. Batch, repeated batch and continuous degradation of Reactive Black 5 and Reactive Red 120 dye by immobilized bacteria. J. Sci. Ind. Res. 71, 504–510.

Varjani, S., Rakholiya, P., Ng, H.Y., You, S., Teixeira, J.A., 2020. Microbial degradation of dyes: an overview. Bioresour. Technol. 314,. https://doi.org/10.1016/j.biortech.2020.123728 123728.

Vinayak, A., Singh, G.B., 2022. Synthetic azo dye bio-decolorization by Priestia sp. RA1: process optimization and phytotoxicity assessment. Arch. Microbiol. 204, 318. https://doi.org/10.1007/s00203-022-02931-9.

Wang, X., Cheng, X., Sun, D., 2008. Autocatalysis in Reactive Black 5 biodecolorization by Rhodopseudomonas palustris W1. Appl. Microbiol. Biotechnol. 80, 907–915. https://doi.org/10.1007/s00253-008-1657-1.

Wanyonyi, W.C., Onyari, J.M., Shiundu, P.M., Mulaa, F.J., 2019. Effective biotransformation of Reactive Black 5 Dye Using Crude Protease from Bacillus Cereus Strain KM201428. Energy Procedia 157, 815–824. https://doi.org/10.1016/j.egypro.2018.11.247.

Wu, J., Han, J., Mao, Y., Wang, L., Wang, Y.i., Li, Y., Wang, Y., 2022. Bionic mineralization growth of UIO-66 with bovine serum for facile synthesis of Zr-MOF with adjustable mesopores and its application in enzyme immobilization. Sep. Purif. Technol., 121505 https://doi.org/10.1016/j.seppur.2022.121505.

Zhang, A., Wang, G., Gong, G., Shen, J., 2017. Immobilization of white rot fungi to carbohydrate-rich corn cob as a basis for tertiary treatment of secondarily treated pulp and paper mill wastewater. Ind. Crops Prod. 109, 538–541. https://doi.org/10.1016/j.indcrop.2017.09.006.

Zille, A., 2005. Laccase Reactions for Textile Applications. Universidade do Minho, Braga, Portugal.